RSC Sustainability

ROYAL SOCIETY OF CHEMISTRY

PAPER

View Article Online
View Journal | View Issue

Cite this: *RSC Sustainability*, 2023, **1**, 335

Upcycling of textile waste into high added value cellulose porous materials, aerogels and cryogels†

Marion Négrier,[a] Elise El Ahmar,[b] Romain Sescousse,[c] Martial Sauceau[c] and Tatiana Budtova *[a]

Cellulose textile waste was upcycled into highly porous and lightweight cellulose materials. Fabrics made of cotton and regenerated cellulose were dissolved in ionic liquids, 1-ethyl-3-methyl imidazolium acetate ([EMIM][OAc]) or 1,5-diazabicyclo[4.3.0]non-5-enium acetate ([DBNH][OAc]), each mixed with dimethyl sulfoxide (DMSO). Non-solvent induced phase separation triggered by ethanol was used to obtain alcogels, which were dried either with supercritical CO_2, or ethanol was exchanged with water and hydrogels were freeze-dried. Alcogels were also atmospheric pressure dried for comparison. Microcrystalline cellulose was used as a reference and processed in the same way. Materials with various porosities and morphologies were obtained. The influence of the cellulose molecular weight, the type of solvent and the drying route on materials' density, porosity, specific surface area and morphology was investigated. The importance of the coagulation pathway, or the way of demixing (instantaneous or delayed), is demonstrated as it allows us to significantly vary the material morphology.

Received 28th October 2022
Accepted 10th January 2023

DOI: 10.1039/d2su00084a

rsc.li/rscsus

Sustainability spotlight

The growth of population requires more textiles, generating more and more waste. Textile recycling (reuse and reprocessing) involves only 20% of the global textile waste. As far as cellulose-based textile waste is concerned, the only upcycling option till now has been spinning "new" fibers by dissolving cellulose-based waste. Our work is focused on upcycling cellulose-based textile waste: we demonstrate the feasibility of making various high added-value porous materials such as cellulose aerogels. Aerogels are lightweight nanostructured materials with a high internal porous surface area. Aerogels' applications span from engineering (thermal and acoustic insulation) to electrochemistry (batteries and fuel cells) and biomedical (delivery matrices and scaffolds). Our work aligns with two UN sustainable development goals: "industry, innovation and infrastructure" and "responsible consumption and production".

1. Introduction

The global textile production is increasing every year, reaching 109 million tons in 2020 with the highest production volumes dedicated to polyester (52%) and cotton fibers (24%).[1] In addition to negative environmental impacts from cotton growing and processing, microplastic pollution directly impacts the quality of life and diminishes biodiversity through soil erosion.[2,3] The growth of population and the improvement of living standards will require more textile fibers, which will generate more and more textile waste, in particular due to the "fast fashion" trend. The majority of textile waste is buried in landfills or burnt. Textile recycling (reuse and reprocessing) makes only 20% of the global textile waste, which was 92 million tons in 2015.[4] Most of the textile waste recycling corresponds to downcycling, *i.e.* fabrication of low value-added materials (mattress fillers and insulation materials).[5] As far as cellulose-based textile waste is concerned, the upcycling options considered till now have been dissolving cellulose-based waste and spinning fibers or casting films; this work is supported by research projects and exists on university laboratory scale[6,7] or performed by small companies.[8,9] In this work we focus on cellulose-based textile waste, and we demonstrate that it is possible to make various high added-value porous materials, in particular, cellulose aerogels.

Aerogels are dry open-pores networks with high porosity (above 90%), interconnected pores, nanostructured and a high specific surface area (at least 100 $m^2\ g^{-1}$).[10] Aerogels based on natural polymers (cellulose, starch, pectin, alginate, *etc.*), so-called bio-aerogels, are new materials developed in the 21st century.[11] They possess a similar morphology and properties to inorganic- or synthetic polymer-based aerogels, but are biodegradable and their synthesis does not involve any toxic compounds.[11] Bio-aerogels can be used in numerous potential applications: as delivery matrices or scaffolds in bio-medical

[a]*Mines Paris, PSL University, Center for Materials Forming (CEMEF), UMR CNRS 7635, CS 10207, Sophia Antipolis, 06904, France. E-mail: tatiana.budtova@minesparis.psl.eu*

[b]*Mines Paris, PSL University, Centre for Thermodynamics of Processes (CTP), Fontainebleau, 77300, France*

[c]*IMT Mines Albi, UMR CNRS 5302, Centre RAPSODEE, Université de Toulouse, 81013 Albi, France*

† Electronic supplementary information (ESI) available. See DOI: https://doi.org/10.1039/d2su00084a

applications and pharmaceutics,[12] in food for the delivery of nutrients, as fat replacers and also for packaging,[13] for thermal insulation and super-insulation,[14] as a catalyst and catalyst support,[15] in electrochemistry when pyrolyzed[16] and for adsorption, absorption and separation.[17]

Cellulose is the most abundant natural polymer on the earth. There are two main ways to make cellulose aerogels: either from native cellulose, based on cellulose I (nanocellulose)[18] or *via* dissolution–coagulation, based on cellulose II.[19] In both cases, in order to achieve a high specific surface area, drying of "wet" cellulose is performed with supercritical CO_2. In the following, we will focus on cellulose II aerogels as nanocellulose-based porous materials are not in the scope of the work. Till now, the majority of publications on cellulose II aerogels used microcrystalline cellulose as the starting matter;[19] few report on the properties of cellulose aerogels made by dissolving cotton or dissolving pulps.[20–22] For example, the influence of the cellulose molecular weight, from DP 180 to 1720, on aerogel mechanical properties was analyzed in ref. 20. Aerogels did not break under uniaxial compression reaching densification at 70–80% strain, and the compressive modulus varied from 0.1 to 50 MPa. Only one publication reported on making cellulose aerogels from textile waste, denim.[23] In that case, imidazolium ionic liquids were used for denim dissolution, cellulose was coagulated in water to remove the solvent, water was exchanged with ethanol and samples were dried under supercritical conditions. In some cases, in addition to small macropores and mesopores that are specific to the aerogel morphology, micron-size tunnels were obtained but the mechanism of their formation was not clarified. Density was not reported and the specific surface area varied from 260 to 390 $m^2\ g^{-1}$.

In this work, we perform an extended study using various post-consumer textile wastes, based on regenerated cellulose (two viscose-based samples) and cotton, to make cellulose aerogels. Microcrystalline cellulose (MCC) was used as a reference. The solvents were two ionic liquids: either standard imidazolium-based, 1-ethyl-3-methylimidazolium acetate ([EMIM][OAc]), or new, 1,5-diazabicyclo[4.3.0]non-5-enium acetate ([DBNH][OAc]).[6] The latter was used as the synthesis is simple, it is much cheaper than [EMIM][OAc] and can be recycled to 95.6%.[24] As [DBNH][OAc] is a solid at room temperature, each ionic liquid was mixed with DMSO to decrease energy for cellulose dissolution. In addition to drying with supercritical CO_2, we performed freeze-drying and drying in a low vacuum; these materials will be called "cryogels" and "xerogels" for simplicity. The morphology, volume shrinkage, density, porosity, pore volume and specific surface area were measured and analyzed for each material. In particular, it was demonstrated that the morphology of materials made from dissolved cotton can be tuned by a phase separation pathway, *i.e.* instantaneous *vs.* delayed demixing.

2. Materials and methods

2.1. Materials

Four types of cellulose were used: microcrystalline cellulose (MCC) Avicel® PH-101 purchased from Sigma Aldrich, and cellulose-based waste fabrics kindly provided by Commitment Fashion and made of cotton or regenerated cellulose named "viscose" and "rayon". Both types of fibers are made from viscose as the starting matter;[25] however, the name of the textile given by the supplier will be kept for a better clarity as cellulose is of different molecular weight (see the Results section).

Ionic liquid 1-ethyl-3-methyl imidazolium acetate ([EMIM][OAc]) was purchased from Iolitec. 1,5-Diazabicyclo[4.3.0]non-5-ene (DBN) was purchased from Fluorochem. Glacial acetic acid (purity > 99%) and dimethyl sulfoxide (DMSO) were from Fisher Scientific. Absolute ethanol (purity > 99%) was purchased from Fisher Chemicals. Water was distilled. All chemicals were used as received.

2.2. Methods

2.2.1. Determination of the cellulose degree of polymerization (DP). The intrinsic viscosity $[\eta]$ (mL g^{-1}) of each cellulose was measured by cellulose dissolution in cupriethylenediamine (CED), following the SCAN-CM standard 15:88 containing the requirements of the ISO 5351. A LAUDA iVisc equipped with an Ubbelohde-type viscometer was used. The molecular weight M (or degree of polymerization) was determined from the Mark–Houwink–Sakurada equation:

$$[\eta] = K \times M^a = K' \times \mathrm{DP}^a \quad (1)$$

where M is the molecular weight and a and K are empirical constants. We used $K' = 0.606$ mL g^{-1} and $a = 0.90$ reported by Evans and Wallis.[26]

2.2.2. Synthesis of the ionic liquid. The ionic liquid ([DBNH][OAc]) was synthesized before each experiment. Glacial acetic acid and DBN were mixed in an equimolar ratio.[27] As the reaction is exothermal, acetic acid was slowly added to DBN under magnetic stirring and a cold-water bath was used to keep the temperature below 30 °C. After all acetic acid was added, the mixture was heated at 70 °C for 1 h to ensure a complete reaction between the reagents. The obtained [DBNH][OAc] was transparent-orange; it was characterized using ^{1}H NMR in DMSO-d_6. The spectra were collected by using a Bruker 400 MHz and showed the same results as reported elsewhere[24] (see Fig. S1 in the ESI†).

2.2.3. Cellulose dissolution and preparation of aerogels, cryogels and xerogels. The preparation of cellulose samples is shown in Fig. 1. Textiles were cut into 1–2 cm pieces, which were further separated into fibers using a mixer. MCC and each textile sample were dried at 50 °C under vacuum for 3 hours. MCC, rayon, viscose and cotton were each dissolved at 5% wt/wt in 50/50 wt/wt [EMIM][OAc]/DMSO or in [DBNH][OAc]/DMSO by magnetic stirring at 300 rpm for 24 h for MCC, rayon and viscose, and by mechanical stirring with a Heidolph RZR 50 overhead mixer at 30 rpm for 24 h for cotton; the mechanical mixer was used because of cotton solution high viscosity. The dissolution was performed at room temperature in all cases. 5% cellulose concentration was used being in-between the overlap concentration of MCC in [EMIM][OAc][28] needed to form a self-standing alcogel or hydrogel (Fig. 1) and the concentration leading to not too viscous solutions that are difficult to handle.

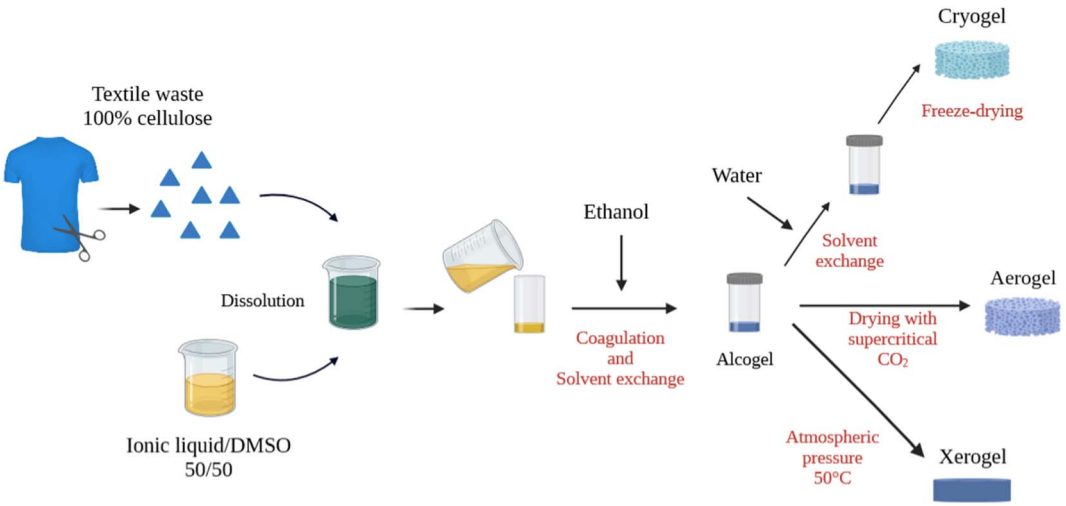

Fig. 1 Schematic presentation of the preparation of cellulose alcogels, aerogels, cryogels and xerogels from textiles. Created with https://biorender.com/.

After complete dissolution, 6 g of cellulose solution were poured in a polypropylene vial or in Soxhlet extraction thimbles that served as molds.

In order to make aerogels using drying with supercritical CO_2, the solvent of cellulose must be replaced by a fluid miscible with CO_2; ethanol was used for this purpose. Ethanol is cellulose non-solvent, and cellulose coagulates forming a 3D network. Coagulation was performed in two ways:

Method 1: direct coagulation.

Ethanol was slowly poured on the top of cellulose/ionic liquid/DMSO solution (Fig. 1). The added volume of ethanol was at least 4 times higher than the volume of the solution. The coagulated sample was washed in ethanol at least 6 times (twice a day) to remove the ionic liquid/DMSO mixture. To ensure a complete replacement of the ionic liquid by ethanol, the electrical conductivity of the bath was checked until it becomes stable at 0.5 μS cm^{-1}. The samples obtained in ethanol, alcogels (Fig. 1), were precursors used for various drying routes.

Method 2: Soxhlet extraction thimbles aided coagulation inspired by ref. 22. Thimbles, that are cellulose-based, were pre-soaked in ethanol, cellulose/ionic liquid/DMSO solution was poured inside and the whole was placed in an ethanol bath. The porous structure of Soxhlet extraction thimbles enables the diffusion of the solvent (ionic liquid/DMSO) out and non-solvent (ethanol) in the sample. After cellulose coagulation, washing steps were performed as described in method 1.

As will be demonstrated in the Results section, the method of coagulation did not influence the morphology and properties of dry materials made from low-to-medium DP cellulose: MCC, rayon or viscose. In contrast, macrovoids and channels appeared when method 1 was used to coagulate dissolved cotton. Thus, the coagulation method will be each time specified.

Aerogels were made by drying the alcogel with supercritical CO_2 following the procedure described elsewhere.[29,30] Briefly, alcogels were placed in a 1 L autoclave, pressurized at 50 bar and 37 °C and ethanol purged. Then, the pressure was increased to 80 bar to reach the supercritical conditions. The system was kept under these conditions for 1 h with an output of 5 kg of CO_2 per h to perform a dynamic washing and remove the remaining ethanol from the alcogel. After this cycle, the system was left in a static mode for 1–2 h and another dynamic cycle of washing of 2 h was launched. The depressurization was carried out with a ramp of 4 bar h^{-1} at 37 °C.

To prepare so-called cryogels, ethanol in alcogels was replaced by water by several washing steps. The samples were then covered with a few millimeters of distilled water and rapidly frozen with liquid nitrogen (−196 °C) for 10 min. The frozen samples were immediately placed in a freeze dryer Cryotec Cosmos 80 for 48 h. This device was preset with water sublimation conditions, which correspond to −80 °C and a primary vacuum at 10 mtorr.

The so-called xerogels were obtained *via* drying the alcogel in an oven at 50 °C under atmospheric pressure for 48 h. The samples were placed on a raised grid for homogeneous evaporation.

After each drying route, the dried samples were stored under low vacuum in a desiccator.

2.2.4. Materials' characterization. The volume shrinkage during the preparation of cellulose materials was calculated as follows:

$$\text{Shrinkage } (\%) = \left(1 - \frac{V_{\text{final}}}{V_{\text{initial}}}\right) \times 100 \quad (2)$$

where V_{initial} and V_{final} are the volumes of the initial cellulose solution and the dried material, respectively. Volumes were determined in two ways: (i) using a Geopyc 1360 envelope density analyzer with DryFlo powder, a chamber of 19.1 mm diameter with an applied force of 27 N, and (ii) with a high-precision caliper. The reason for measuring the sample volume with two methods is that for cotton-based samples made with method 1 DryFlo powder partially penetrated the

channels, thus potentially decreasing the sample total volume, and manual measurement of samples with a distorted shape is not precise. In the following, the volumes and the corresponding samples' density, porosity and pore volume will be referred to as "Geopyc" and "manual". For these two methods, the experimental errors do not exceed 3% and 10%, respectively.

The bulk density (ρ_{bulk}) was determined as the ratio of sample mass (m) to volume (V_{final}):

$$\rho_{bulk}\left(\text{g cm}^{-3}\right) = \frac{m}{V_{final}} \quad (3)$$

The porosity and the theoretical specific pore volume V_{pores} were calculated from the bulk and the skeletal density (ρ_{sk}) of cellulose (the latter taken as 1.5 g cm^{-3} (ref. 31)), as follows:

$$\text{Porosity } (\%) = \left(1 - \frac{\rho_{bulk}}{\rho_{sk}}\right) \times 100 \quad (4)$$

$$V_{pores}\left(\text{cm}^3\ \text{g}^{-1}\right) = \frac{1}{\rho_{bulk}} - \frac{1}{\rho_{sk}} \quad (5)$$

The specific surface area (S_{BET}) was measured with an ASAP 2020 high-performance adsorption analyzer from Micromeritics using the nitrogen adsorption technique and Brunauer–Emmett–Teller (BET) theory. The samples were first degassed under high vacuum at 70 °C for 12 h. The average error was below 20 m^2 g^{-1}.

To investigate the morphology of the obtained dried cellulose materials, they were placed in liquid nitrogen, broken and cross sections were analysed with scanning electron microscopy (SEM) using a MAIA 3 (Tescan) equipped with detectors of secondary and back-scattered electrons. A 14 nm layer of platinum was applied with a Q150T Quorum metallizer in order to prevent the accumulation of electrostatic charges and images' defaults. The observations were done with the acceleration voltage set at 3 kV.

3. Results and discussion

3.1. Determination of cellulose DP

The reduced viscosity as a function of concentration for all cellulose samples dissolved in CED is shown in Fig. S2.† Intrinsic viscosity values and the corresponding DP (see the Methods section) are presented in Table 1. The DP of MCC is 248 and is consistent with the values reported in the literature.[27,32,33] For rayon and viscose, the cellulose DP is 372 and 413, respectively, also matching well the values known in the literature, between 300 and 450.[34] The DP of cotton is much higher, 1591, as expected.[35]

3.2. Visual appearance of cellulose materials, shrinkage, density, porosity and pore volume

The representative photos of the aerogels, cryogels and xerogels based on different celluloses dissolved in [DBNH][OAc]/DMSO and in [EMIM][OAc]/DMSO are shown in Fig. 2 and S3,† respectively; the shape of the samples is not influenced by the solvent used. Fig. S4† shows the examples of alcogels of cellulose dissolved in [EMIM][OAc]/DMSO, and the same appearance was observed for alcogels of cellulose dissolved in [DBNH][OAc]/DMSO. Aerogels and cryogels from MCC, rayon and viscose (Fig. 2 and S3†) have a regular shape of disks reflecting the shape of the vials or the Soxhlet thimbles (Fig. S5†) where cellulose solutions were coagulated. Cryogels often have some cracks, most probably because of the internal stresses developed due to the growth of ice crystals (Fig. 2 and S3†). The volume of xerogels from all celluloses is significantly lower than that of aerogels and cryogels (Fig. 2 and S3†).

The shape of all samples from cotton is distorted when made using coagulation method 1 (Fig. 2 and S3†) and is regular when made using coagulation method 2 (Fig. S5†). In addition, aerogel and cryogel obtained with method 1 have large finger-like macrovoids (Fig. S6†). Fingering is a known phenomenon occurring during membrane preparation, for example, when a membrane is formed from a polymer solution *via* phase separation processes.[36] The same phenomenon was also reported for cellulose (kraft pulp) dissolved in NMMO monohydrate and coagulated in water[37] and in some aerogels based on cotton dissolved in imidazolium ionic liquids and coagulated in water.[23] The formation of "fingers" during the phase inversion (polymer solution in contact with a non-solvent) is explained as follows. First, a skin layer is formed due to the instantaneous liquid–liquid demixing. Due to the heterogeneities in the skin layer, a low-viscosity non-solvent (in our case, ethanol) displaces cellulose solution and creates flow instabilities. Cellulose-poor phase displaces cellulose solution and forms fingers. Within a finger, the exchange of solvent and non-solvent is much faster than through the skin, resulting in a fast propagation of the coagulation front within a finger. The presence of fingers results in strong inhomogeneities of density along the sample, and consequently, in the development of internal stresses within the coagulating cellulose. As a result, the shape of samples based on dissolved cotton is distorted.

It is known that polymer membranes with macrovoids are formed in the case of instantaneous demixing; a delayed demixing usually results in a so-called "sponge-like" homogeneous morphology.[38] It is also known that, in general, higher viscosity of polymer solution should lead to a delayed demixing, thus preventing the initiation of fingers.[36] In our study, an opposite result was obtained: materials based on coagulated cellulose of

Table 1 Intrinsic viscosity and DP of all celluloses used in the work

Cellulose source	MCC	Rayon	Viscose	Cotton
Intrinsic viscosity, mL g^{-1}	86.5 ± 1.7	124.8 ± 2.5	137 ± 2.7	461.4 ± 9.2
DP	248 ± 5	372 ± 7	413 ± 8	1591 ± 32

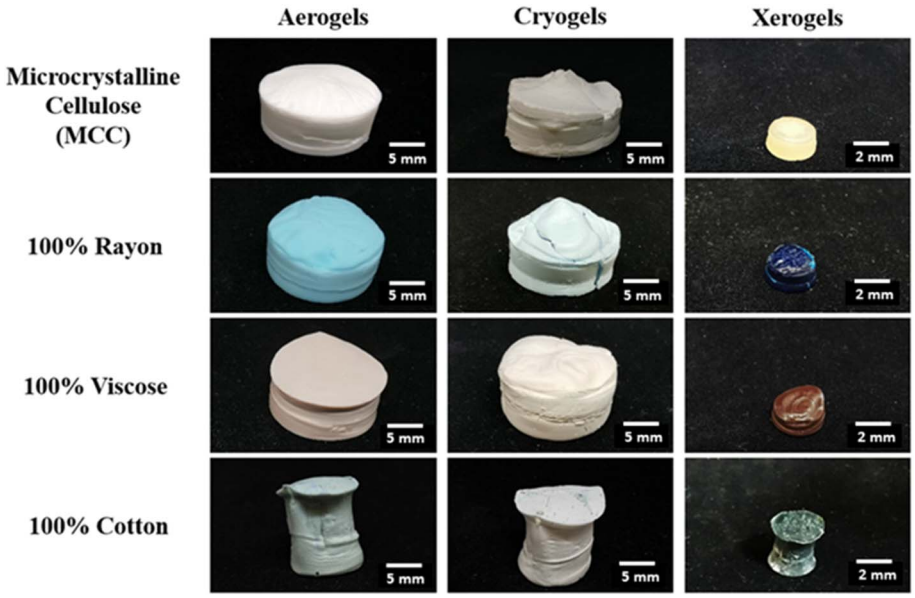

Fig. 2 Photos of cellulose aerogels, cryogels and xerogels from MCC and cellulose from textiles. The solvent was [DBNH][OAc]/DMSO and cellulose solutions were coagulated according to method 1.

lower molecular weight (solutions are less viscous) are homogeneous and cotton-based materials are with macrovoids; a similar result with vertical "tunnels" was observed for cellulose aerogels produced from cotton[23] but demixing features were not considered. The result obtained might be due to the difference in the relaxation of macromolecules of different molecular weights during coagulation. Cellulose of lower DP relaxes quickly (equivalent to the relaxation to a glassy state) and high-DP cotton relaxes slowly, which induces heterogeneities in the skin layer opening the way for the formation of fingers. When using method 2 for coagulation, a "barrier" of Soxhlet thimbles leads to a strong delay in demixing, resulting in homogeneous cotton-based materials. Another way to avoid the formation of macrovoids and channels is to coagulate cellulose in a mixture of a solvent and non-solvent: when we coagulated dissolved cotton in a mixture of ethanol/[DBNH][OAc]/DMSO, no macrovoids were observed. These results are not discussed as such coagulation process takes a long time and uses a larger amount of ionic liquid.

Polymer chains contract when placed in a non-solvent, and thus the volume of all dry cellulose samples was lower than the volume of the corresponding solutions. The total shrinkage (eqn (2)) is presented in Fig. 3 for both solvents used to dissolve MCC and textiles. Samples obtained with only coagulation

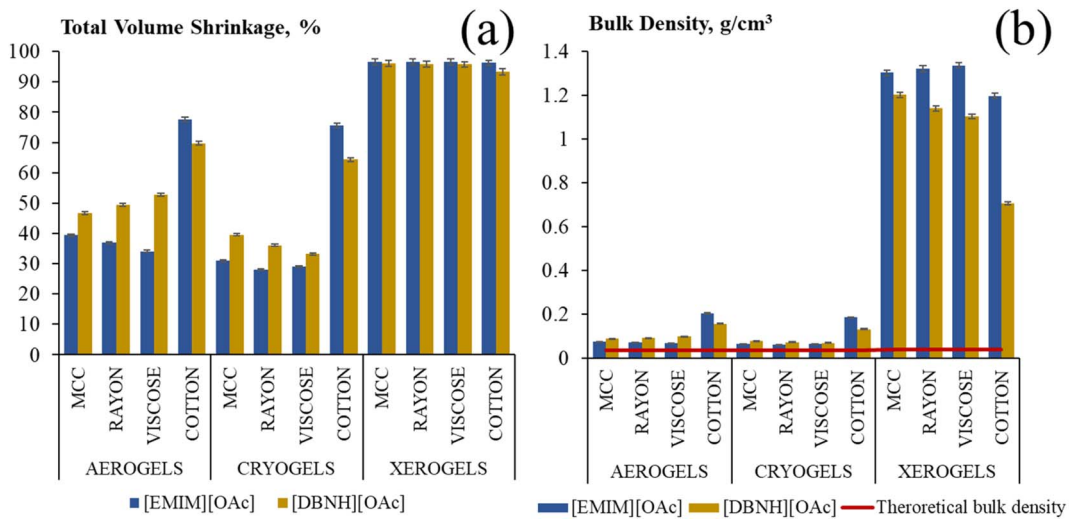

Fig. 3 Total volume shrinkage (a) and bulk density (b) of all aerogels, cryogels and xerogels made using [DBNH][OAc]/DMSO and [EMIM][OAc]/DMSO and method 1 for cellulose coagulation. Volume and density were determined with Geopyc. The red line in (b) corresponds to a theoretical density calculated supposing no shrinkage.

method 1 are shown and the volume was determined with Geopyc. Shrinkage during the preparation of aerogels or cryogels is similar for samples based on dissolved MCC, rayon and viscose and is higher for those based on cotton (Fig. 3). The volume shrinkage increased in the following order: cryogels (30–40%) < aerogels (40–75%) < xerogels (90–95%); the same trend was reported in ref. 39. When cryogels are made, the sample shrinks only during solvent exchange, from solution to alcogel. For aerogels, the shrinkage occurs during coagulation and also during drying with supercritical CO_2 as the Hansen solubility parameter of the latter strongly differs from the one of cellulose: $\delta = 17.4$ MPa$^{1/2}$ for CO_2 (ref. 40) *vs.* $\delta = 38.6$ MPa$^{1/2}$ for cellulose (see details on solubility parameter in Table S1†). For both solvents, the shrinkage of xerogels is the highest (Fig. 3a) because of pores' collapse due to the capillary pressure arising during evaporative drying.

The influence of coagulation method (method 1 *vs.* method 2) on the shrinkage is shown in Fig. S7.† In most cases, aerogels and cryogels coagulated in Soxhlet thimbles (method 2) have slightly lower shrinkage than that when samples were directly coagulated using method 1. We suppose that sample heterogeneity and formation of a thick skin during direct addition of a non-solvent might be the reason for higher shrinkage when using coagulation method 1.

Finally, the comparison of two ways of measuring sample volume, manually and with Geopyc, is presented in Fig. S8† for the samples made from cotton using method 1. As expected, shrinkage values obtained with Geopyc are slightly higher than those determined manually as the volumes obtained with Geopyc are underestimated because DryFlo powder partially penetrates large pores, thus artificially decreasing the sample volume. To summarize, the trends obtained are the same whatever is the coagulation method used or way of measuring the volume; however, the absolute values are different. This result has never been discussed in the literature and should be considered when comparing results from different laboratories.

The bulk density of the prepared materials (Fig. 3b) correlates with their volume shrinkage; in all cases the density is higher than the estimated which was calculated supposing no shrinkage (red line in Fig. 3b). The highest bulk densities are observed for xerogels, from 1.19 to 1.33 g cm^{-3} when the solvent was [EMIM][OAc]/DMSO and slightly lower, from 0.7 to 1.2 g cm^{-3}, when the solvent was [DBNH][OAc]/DMSO. Xerogels from cotton dissolved in [DBNH][OAc]/DMSO had the lowest density, around 0.7 g cm^{-3}, measured with Geopyc. It may be possible that large macrovoids do not collapse completely as the capillary pressure is inversely proportional to the pore diameter. Aerogels and cryogels had very low densities, between 0.06 and 0.2 g cm^{-3}, with cryogels possessing the lowest values (0.06–0.13 g cm^{-3}) because of the lowest shrinkage (Fig. 3b). Samples from dissolved cotton shrink more during coagulation as compared to low-molecular weight cellulose (compare the densities of aero- and cryogels in Fig. 3b) but less during drying at atmospheric pressure (compare the densities of xerogels in Fig. 3b). Overall, aerogels and cryogels from dissolved cellulose-based textiles have similar densities as compared to those of dissolved neat cellulose, MCC, whatever is the ionic liquid used and the way of coagulation used.

The porosity of all samples calculated with eqn (4) is shown in Fig. 4a. It is around and higher than 90% for aerogels and cryogels made from both ionic liquids. Xerogels' porosity is much lower, as expected from the values of density, around 20% when [EMIM][OAc]/DMSO was used and around 50% for the case of [DBNH][OAc]/DMSO. An increase of the xerogels' porosity is observed with the increase of the cellulose molecular weight, from 20% for MCC up to 50% for cotton when [DBNH][OAc]/DMSO was used as solvent. As mentioned above, the reason can be the preservation of macrovoids during atmospheric pressure drying.

The pore volume (eqn (5)) of aerogels and cryogels obtained by MCC, rayon and viscose dissolution in both ionic liquids is between 9 and 15 cm^3 g^{-1}, and it is lower for dissolved cotton,

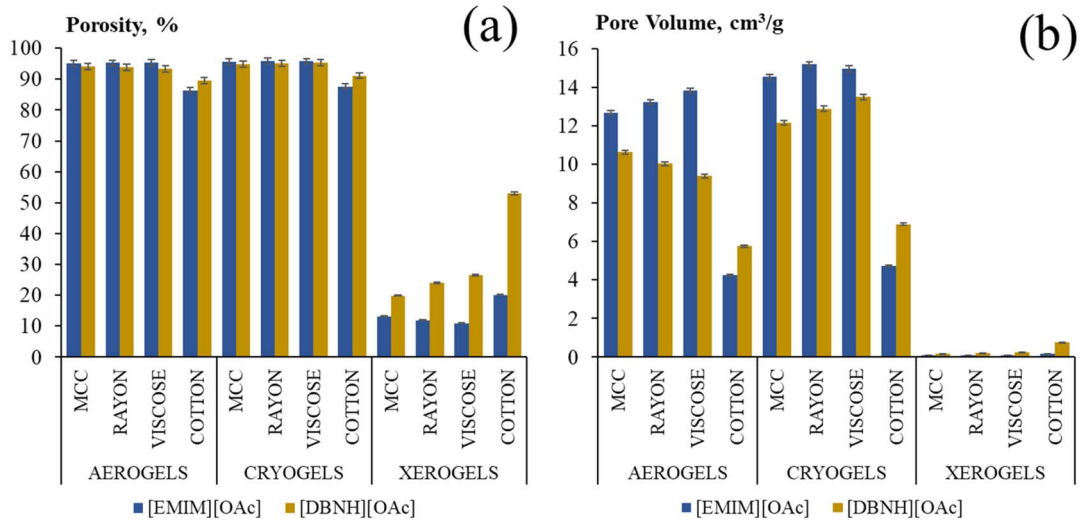

Fig. 4 Porosity (a) and pore volume (b) of all aerogels, cryogels and xerogels made using [DBNH][OAc]/DMSO and [EMIM][OAc]/DMSO and method 1 for cellulose coagulation. Volume and density were determined with Geopyc.

around 4–6 $cm^3\ g^{-1}$ (Fig. 4b); similar values were obtained with coagulation method 2 (Fig. S7†). All xerogels have a very low pore volume, below 1 $cm^3\ g^{-1}$, as expected from their higher density.

3.3. Specific surface area and morphology

For xerogels, the values of the specific surface area were too low to be accurately determined. The ones of aerogels and cryogels are shown in Fig. 5 for the samples made with coagulation method 1. The values obtained with method 2 are the same as with method 1 within the experimental errors (Fig. S7e†) due to the fact that the "input" of macrovoids into the surface area is low. Whatever is the ionic liquid and the coagulation method used, the surface area of aerogels is higher than that of cryogels, 320–400 $m^2\ g^{-1}$ *vs.* 10–100 $m^2\ g^{-1}$, respectively. For cryogels, the surface area increases with the increase of the cellulose molecular weight (from 12 to 104 $m^2\ g^{-1}$ and from 12 to 33 $m^2\ g^{-1}$ when using [EMIM][OAc]/DMSO and [DBNH][OAc]/DMSO, respectively); a similar trend was reported for neat celluloses.[20]

The inner morphology of the materials was analyzed by SEM (Fig. 6 and S9† for materials made using [DBNH][OAc]/DMSO and [EMIM][OAc] as solvent, respectively, and Fig. S10 and S11† for some xerogels). Aerogels and cryogels are open-pore materials but their morphology strongly depends on the drying route. The inner structure of aerogels consists of beads assembled in a network, and the beads themselves are made of a network of fine cellulose "fibrils" with a pore size of 10–200 nm (Fig. 6 and S9†). Such a bead-like morphology had already been reported for cellulose aerogels made using [EMIM][OAc] as solvent,[21,39,41] and it is the same for aerogels made using [DBNH][OAc]. It was suggested that the bead-like network structure is formed due to spinodal decomposition-governed phase separation occurring when a non-solvent is added to cellulose "liquid" solution.[41] A similar morphology was reported for cellulose coagulated from hot (or molten) cellulose-NMMO monohydrate solution.[37] Indeed, the nucleation and growth mechanism, which is often reported for membranes, cannot explain the formation of regular "micro-beads" of the same size. As discussed previously, the coagulation method did not influence the aerogel morphology except when cotton was used and finger-like macrovoids were formed (see Fig. S3†).

The pores of cryogels are of a few microns and have rather flat continuous pore walls. Such a morphology is formed as a compromise between the growth of ice crystals pushing and deforming the pores of the cellulose hydrogel and the "resistance" of the cellulose network formed during coagulation. The increase of the cellulose molecular weight leads to the decrease of pore size in cryogels, and pore walls become porous (compare SEM images in Fig. 6B for cryogels made from MCC and in Fig. 6H for cryogels from cotton): a higher molecular weight increases network "resistance" to the mechanical stresses arising during the growth of ice crystals under freezing. This evolution of the morphology correlates well with the increase of cryogels' specific surface area with the cellulose molecular weight (Fig. 5).

As expected from Fig. 4, the morphology of xerogels shows low porosity (Fig. S10 and S11†) whatever was the solvent used.

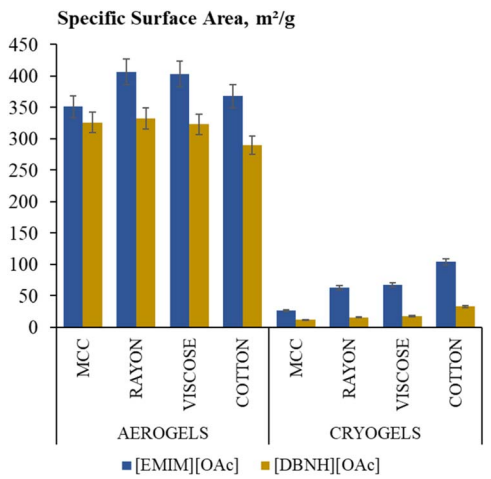

Fig. 5 Specific surface area of all aerogels and cryogels made using [DBNH][OAc]/DMSO and [EMIM][OAc]/DMSO and coagulation method 1.

4. Discussion

Numerous results have been presented in this paper; the main trends are summarized and discussed below:

(a) Influence of the cellulose type and molecular weight on the morphology and properties of aerogels and cryogels.

For cellulose of a similar DP the type of cellulose allomorph (cellulose I: here, MCC, and cellulose II: here, viscose and rayon) does not influence the aerogel properties and morphology. The same conclusion applies to cryogels. This means that textile waste based on cellulose II, which usually has a medium DP, can be easily used for making aerogels and cryogels.

When cotton (high DP) was dissolved in an ionic liquid, channels and macrovoids (so-called "fingers") were formed during direct coagulation due to instantaneous demixing. Such aerogels and cryogels had heterogeneous density; the development of internal stresses during coagulation resulted in samples with a distorted shape. However, the "bulk" morphology (outside the macrovoids) was aerogel-like or cryogel-like depending on the drying method. This particular hierarchical morphology can be an interesting way to make membranes with pores of several hundreds of microns and porous walls with pores of some tens of nanometers. For obtaining samples with a homogeneous morphology, the principle of delayed demixing should be applied; to do this, we placed dissolved cotton in soxhlet thimbles imbibed with a non-solvent, ethanol.

Another example of the influence of cellulose DP on material properties was recorded for cryogels: a higher molecular weight resulted in a higher specific surface area, which was in particular high for cryogels reaching 100 $m^2\ g^{-1}$. Cellulose with a high DP (here, cotton) better "resists" the growth of ice crystals under freezing resulting in a material of low density but with smaller pores, and thus a higher surface area.

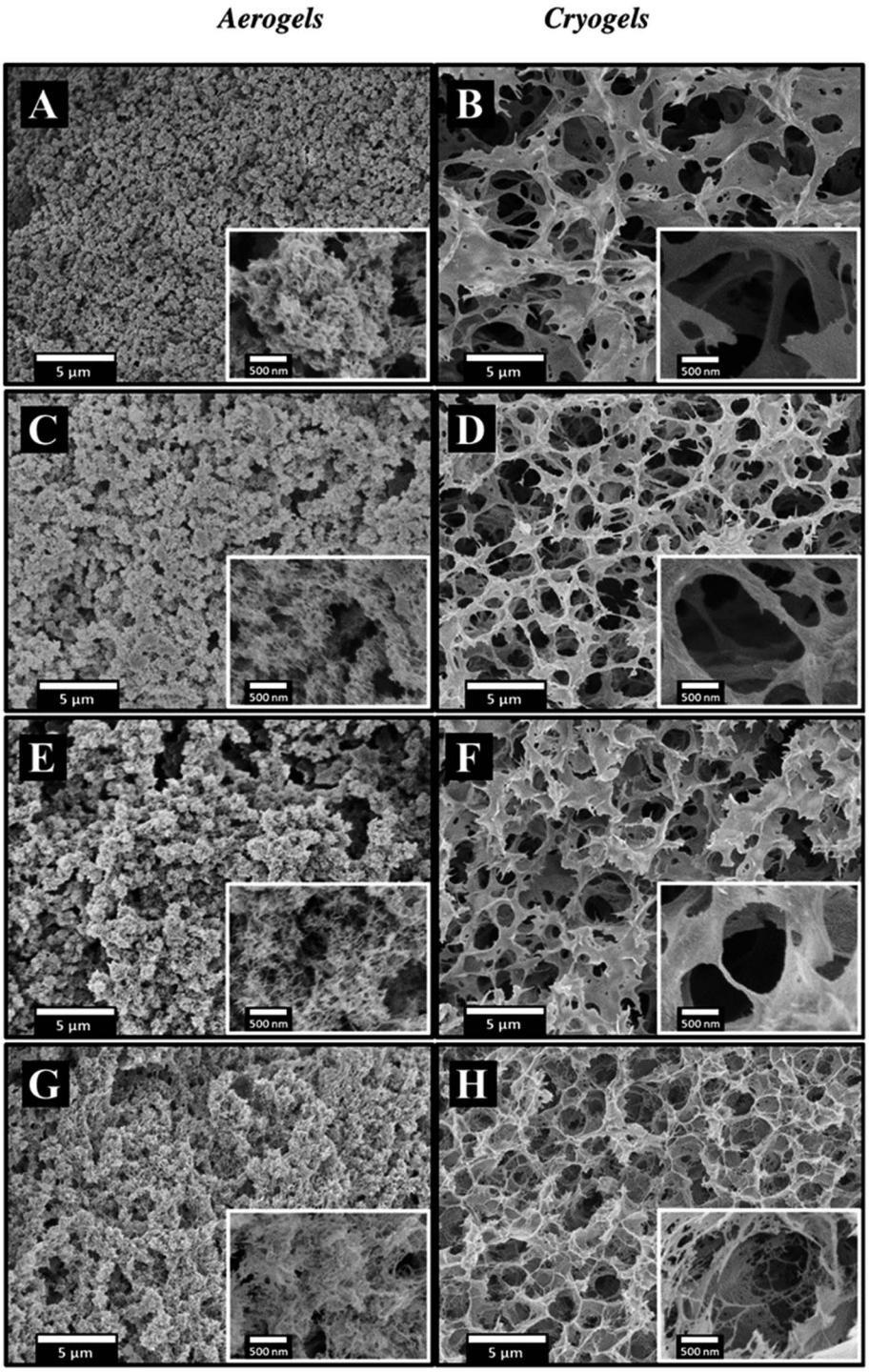

Fig. 6 Morphology of aerogels (A, C, E and G) and cryogels (B, D, F and H) from MCC (A and B), rayon (C and D), viscose (E and F) and cotton (outside macrovoids) (G and H) dissolved in [DBNH][OAc]/DMSO and coagulated using method 1.

(b) Influence of the cellulose type and molecular weight on xerogel properties.

It is well known that in most cases, the pores in "wet" cellulose (coagulated cellulose with non-solvent in the pores, sometimes called alcogels or hydrogels) collapse if dried at atmospheric pressure. The reason is high capillary pressure which depends on the liquid/gas surface tension, liquid/solid contact angle and pore diameter. The smaller the pores, the higher the capillary pressure, and thus cellulose alcogels based on medium-DP cellulose collapse under ambient-pressure drying. No influence of the cellulose allomorph type was recorded. When high-DP cellulose (cotton) was used, macrovoids and channels (formed when dissolved cotton was directly coagulated in ethanol) preserved certain porosity of

atmospheric-pressure dried cellulose: samples with 50% porosity were obtained. However, because the small pores collapsed, the specific surface area was very low (below the detection limit). Higher cellulose DP also reinforced the network pore walls in alcogels resulting in lower shrinkage during evaporative drying as compared with medium-DP based cellulose. The xerogels obtained were less dense than the ones obtained from medium-DP cellulose.

(c) Influence of solvent on aerogel and cryogel properties.

In this work, two different ionic liquids, [EMIM][OAc] and [DBNH][OAc], each mixed with DMSO, were used to make porous cellulose materials, aerogels and cryogels. DMSO was used as a "co-solvent" to have cellulose solutions in the liquid state at room temperature. We showed that as soon as dissolved cellulose is coagulated from a "liquid state", the type of ionic liquid does not significantly influence the properties of porous cellulose. For both solvents, the morphology of aerogels was a network of assembled porous beads which we interpret as a result of phase separation governed by spinodal decomposition.

5. Conclusions

Textile waste – rayon, viscose and cotton – was recycled into ultralight and highly porous materials, aerogels and cryogels. The textile was fully dissolved in ionic liquids, either 1-ethyl-3-methyl imidazolium acetate ([EMIM][OAc]) or 1,5-diazabicyclo [4.3.0]non-5-enium acetate ([DBNH][OAc]), each mixed with DMSO, and placed in ethanol to induce phase separation. Different drying routes were applied: with supercritical CO_2, freeze-drying and atmospheric pressure drying. Microcrystalline cellulose was used as a reference and processed in the same way as textiles. Two ways of liquid–liquid demixing, instantaneous and delayed, were used.

The molecular weight of low to medium DP of cellulose (MCC, rayon and viscose) and phase separation pathway (instantaneous or delayed demixing) did not significantly influence the morphology and properties of aerogels, cryogels and xerogels. Aerogels possessed a bulk density from 0.07 and 0.2 g cm^{-3} and a specific surface area from 300 to 400 m^2 g^{-1}. Cryogels possessed a bulk density of 0.06–0.18 g cm^{-3} and a specific surface area much lower than that of aerogels, from 10 to 100 m^2 g^{-1}. The increase of the cellulose molecular weight increases the cryogel specific surface area. Xerogels had a high density (from 0.7 to 1.3 g cm^{-3}) and a negligible specific surface area due to pores' collapse during atmospheric pressure drying.

It was demonstrated that in the case of high molecular weight cellulose solution (here, cotton), the morphology of materials is strongly influenced by the phase separation pathway, instantaneous or delayed demixing. Instantaneous demixing resulted in materials with large finger-like macrovoids and a distorted shape while delayed demixing resulted in materials that kept the shape of the mould and with a homogeneous morphology.

The method of density (or volume) measurement, which involves a density analyzer or a caliper, resulted in different values in the case of instantaneous demixing of cotton-based materials.

The results obtained show the potential of upcycling textiles into highly porous celluloses with different porosities and morphologies. Their applications depend on the "restrictions" towards additives that remain in the final material; packaging, interior decoration or delivery matrices for fertilizers can be prospective options. The presence of colorants from textiles should not be an obstacle as, by definition, they should not be toxic for the skin.

Conflicts of interest

There are no conflicts of interest to declare.

Abbreviations

MCC	Microcrystalline cellulose
DP	Degree of polymerization
[EMIM][OAc]	1-Ethyl-3-methyl imidazolium acetate
[DBNH][OAc]	1,5-Diazabicyclo[4.3.0]non-5-enium acetate
DMSO	Dimethyl sulfoxide
DBN	1,5-Diazabicyclo[4.3.0]non-5-ene
CED	Cupriethylenediamine
BET	Brunauer–Emmett–Teller
SEM	Scanning electron microscopy
CO_2	Carbon dioxide
ILs	Ionic liquids

Acknowledgements

The authors are grateful to Institut CARNOT M.I.N.E.S for funding. We warmly thank Pierre Ilbizian and Julien Jaxel (PERSEE, Mines Paris) for supercritical drying, Suzanne Jacomet (CEMEF, Mines Paris) for guiding in SEM imaging, Alice Mija (ICN, University of Nice Sophia Antipolis) for help in NMR analysis and Commitment Fashion for providing textiles.

References

1 Preferred Fiber and Materials Market Report – Textile Exchange, 2021, [cited 2022 Jan 25], Available from: https://textileexchange.org/preferred-fiber-and-materials-market-report/.

2 B. Henry, K. Laitala and I. G. Klepp, Microfibres from apparel and home textiles: prospects for including microplastics in environmental sustainability assessment, *Sci. Total Environ.*, 2019, **652**, 483–494.

3 A. P. Periyasamy and A. Tehrani-Bagha, A review on microplastic emission from textile materials and its reduction techniques, *Polym. Degrad. Stab.*, 2022, **199**, 109901.

4 Pulse of the Industry — GLOBAL FASHION AGENDA], [cited 2022 Jan 26], Available from: https://www.globalfashionagenda.com/publications-and-policy/pulse-of-the-industry/.

5 G. Celep, G. D. Tetik and F. Yilmaz, *Limitations of Textile Recycling: the Reason behind the Development of Alternative*

Sustainable Fibers, IntechOpen, 2022, [cited 2022 Jul 29]. Available from: https://www.intechopen.com/online-first/82044.

6 S. Haslinger, M. Hummel, A. Anghelescu-Hakala, M. Määttänen and H. Sixta, Upcycling of cotton polyester blended textile waste to new man-made cellulose fibers, *Waste Manage.*, 2019, **97**, 88–96.

7 G. Xia, W. Han, Z. Xu, J. Zhang, F. Kong, J. Zhang, *et al.*, Complete recycling and valorization of waste textiles for value-added transparent films via an ionic liquid, *J. Environ. Chem. Eng.*, 2021, **9**(5), 106182.

8 *Biomaterials | Nordic Bioproducts Group*, Nordic Bioproducts, [cited 2022 Jul 29], Available from: https://www.nordicbioproducts.fi.

9 *Renewcell*, Renewcell, [cited 2022 Jul 29]. Available from: https://www.renewcell.com/en.

10 M. A. Aegerter, N. Leventis, M. Koebel and S. A. Steiner III, *Handbook of Aerogels*, Springer, 2nd edn, 2023, p. 3050.

11 S. Zhao, W. J. Malfait, N. Guerrero-Alburquerque, M. M. Koebel and G. Nyström, Biopolymer aerogels and foams: chemistry, properties, and applications, *Angew. Chem., Int. Ed.*, 2018, **57**(26), 7580–7608.

12 C. López-Iglesias, J. Barros, I. Ardao, F. J. Monteiro, C. Alvarez-Lorenzo, J. L. Gómez-Amoza, *et al.*, Vancomycin-loaded chitosan aerogel particles for chronic wound applications, *Carbohydr. Polym.*, 2019, **204**, 223–231.

13 L. Manzocco, K. S. Mikkonen and C. A. García-González, Aerogels as porous structures for food applications: smart ingredients and novel packaging materials, *Food Struct.*, 2021, **28**, 100188.

14 F. Zou and T. Budtova, Polysaccharide-based aerogels for thermal insulation and superinsulation: an overview, *Carbohydr. Polym.*, 2021, **266**, 118130.

15 J. Rooke, C. Passos, M. Chatenet, R. Sescousse, T. Budtova, S. Berthon-Fabry, *et al.*, Synthesis and properties of platinum nanocatalyst supported on cellulose-based carbon aerogel for applications in PEMFCs, *J. Electrochem. Soc.*, 2011, **158**, B779–B789.

16 J. Rooke, R. Sescousse, T. Budtova, S. Berthon-Fabry, B. Simon and M. Chatenet, *Cellulose-based nanostructured carbons for energy conversion and storage devices*, 2013, pp. 89–111.

17 H. Zhang, Y. Li, Y. Xu, Z. Lu, L. Chen, L. Huang, *et al.*, Versatile fabrication of a superhydrophobic and ultralight cellulose-based aerogel for oil spillage clean-up, *Phys. Chem. Chem. Phys.*, 2016, **18**(40), 28297–28306.

18 N. Lavoine and L. Bergström, Nanocellulose-based foams and aerogels: processing, properties, and applications, *J. Mater. Chem. A*, 2017, **5**(31), 16105–16117.

19 T. Budtova, Cellulose II aerogels: a review, *Cellulose*, 2019, **26**(1), 81–121.

20 N. Buchtová, C. Pradille, J. L. Bouvard and T. Budtova, Mechanical properties of cellulose aerogels and cryogels, *Soft Matter.*, 2019, **15**(39), 7901–7908.

21 N. Pircher, L. Carbajal, C. B. Schimper, M. Bacher, H. Rennhofer, J. Nedelec, *et al.*, Impact of selected solvent systems on the pore and solid structure of cellulose aerogels, *Cellulose*, 2016, **23**, 1949–1966.

22 S. F. Plappert, J. M. Nedelec, H. Rennhofer, H. C. Lichtenegger, S. Bernstorff and F. W. Liebner, Self-assembly of cellulose in super-cooled ionic liquid under the impact of decelerated antisolvent infusion: an approach toward anisotropic gels and aerogels, *Biomacromolecules*, 2018, **19**(11), 4411–4422.

23 B. Zeng, X. Wang and N. Byrne, Development of cellulose based aerogel utilizing waste denim—A morphology study, *Carbohydr. Polym.*, 2019, **205**, 1–7.

24 A. Parviainen, R. Wahlström, U. Liimatainen, T. Liitiä, S. Rovio, J. K. J. Helminen, *et al.*, Sustainability of cellulose dissolution and regeneration in 1,5-diazabicyclo[4.3.0]non-5-enium acetate: a batch simulation of the IONCELL-F process, *RSC Adv.*, 2015, **5**(85), 69728–69737.

25 I. S. F. Mendes, A. Prates and D. V. Evtuguin, Production of rayon fibres from cellulosic pulps: state of the art and current developments, *Carbohydr. Polym.*, 2021, **273**, 118466.

26 R. Evans and A. F. A. Wallis, Cellulose molecular weights determined by viscometry, *J. Appl. Polym. Sci.*, 1989, **37**(8), 2331–2340.

27 A. Ostonen, J. Bervas, P. Uusi-Kyyny, V. Alopaeus, D. H. Zaitsau, V. N. Emel'yanenko, *et al.*, Experimental and theoretical thermodynamic study of distillable ionic liquid 1,5-diazabicyclo[4.3.0]non-5-enium acetate, *Ind. Eng. Chem. Res.*, 2016, **55**(39), 10445–10454.

28 M. Gericke, K. Schlufter, T. Liebert, T. Heinze and T. Budtova, Rheological properties of cellulose/ionic liquid solutions: from dilute to concentrated states, *Biomacromolecules*, 2009, **10**(5), 1188–1194.

29 S. Groult, S. Buwalda and T. Budtova, Pectin hydrogels, aerogels, cryogels and xerogels: Influence of drying on structural and release properties, *Eur. Polym. J.*, 2021, **149**, 110386.

30 F. Zou and T. Budtova, Tailoring the morphology and properties of starch aerogels and cryogels via starch source and process parameter, *Carbohydr. Polym.*, 2021, **255**, 117344.

31 C. Sun, True density of microcrystalline cellulose, *J. Pharm. Sci.*, 2005, **94**(10), 2132–2134.

32 L. Druel, P. Niemeyer, B. Milow and T. Budtova, Rheology of cellulose-[DBNH][CO2Et] solutions and shaping into aerogel beads, *Green Chem.*, 2018, **20**(17), 3993–4002.

33 J. Rojas, A. Lopez, S. Guisao and C. Ortiz, Evaluation of several microcrystalline celluloses obtained from agricultural by-products, *J. Adv. Pharm. Technol. Res.*, 2011, **2**(3), 144–150.

34 S. J. Kadolph and A. L. Langford, *Textiles*, Pearson Education, 11th edn, 2013, p. 595.

35 L. E. Hessler, G. V. Merola and E. E. Berkley, Degree of polymerization of cellulose in cotton fibers, *Text. Res. J.*, 1948, **18**(10), 628–634.

36 J. Ren and R. Wang, Preparation of polymeric membranes, in *Handbook of Environmental Engineering*, 2010, pp. 47–100.

37 O. Biganska and P. Navard, Morphology of cellulose objects regenerated from cellulose-*N*-methylmorpholine N-oxide–water solutions, *Cellulose*, 2008, **16**, 179–188.

38 A. J. Reuvers and C. A. Smolders, Formation of membranes by means of immersion precipitation: part II. the mechanism of formation of membranes prepared from the system cellulose acetate-acetone-water, *J. Membr. Sci.*, 1987, **34**(1), 67–86.
39 N. Buchtová and T. Budtova, Cellulose aero-, cryo- and xerogels: towards understanding of morphology control, *Cellulose*, 2016, **23**(4), 2585–2595.
40 A. F. M. Barton, *Handbook of Solubility Parameters and Other Cohesion Parameters*, CRC Press, 1991, p. 774.
41 R. Sescousse, R. Gavillon and T. Budtova, Aerocellulose from cellulose–ionic liquid solutions: preparation, properties and comparison with cellulose–NaOH and cellulose–NMMO routes, *Carbohydr. Polym.*, 2011, **83**(4), 1766–1774.